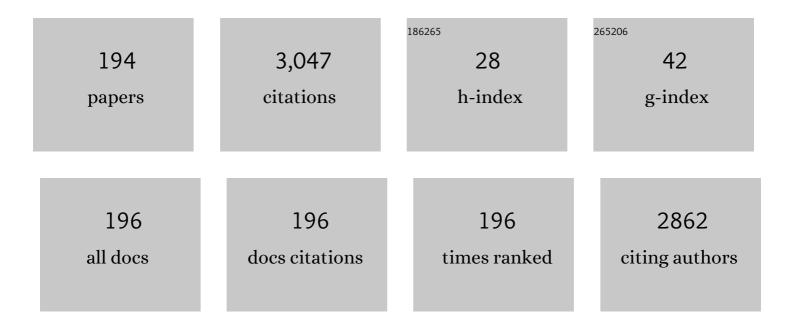
List of Publications by Year in descending order

Source: https://exaly.com/author-pdf/9110208/publications.pdf Version: 2024-02-01



VIIDV SHURIN

#	Article	IF	CITATIONS
1	Low-temperature CO oxidation by Pd/CeO2 catalysts synthesized using the coprecipitation method. Applied Catalysis B: Environmental, 2015, 166-167, 91-103.	20.2	167
2	Influence of Niâ^'Co Catalyst Composition on Nitrogen Content in Carbon Nanotubes. Journal of Physical Chemistry B, 2004, 108, 9048-9053.	2.6	114
3	Copper on carbon materials: stabilization by nitrogen doping. Journal of Materials Chemistry A, 2017, 5, 10574-10583.	10.3	103
4	Ni–Mo and Co–Mo alloy nanoparticles for catalytic chemical vapor deposition synthesis of carbon nanotubes. Journal of Alloys and Compounds, 2015, 621, 351-356.	5.5	77
5	Fluorination of Arc-Produced Carbon Material Containing Multiwall Nanotubes. Chemistry of Materials, 2002, 14, 1472-1476.	6.7	70
6	Title is missing!. Journal of Structural Chemistry, 2003, 44, 46-59.	1.0	54
7	One-pot reductive amination of aldehydes with nitroarenes over an Au/Al <sub>2</sub> O <sub>3</sub> catalyst in a continuous flow reactor. Catalysis Science and Technology, 2015, 5, 4741-4745.	4.1	51
8	Stabilization of active sites in alloyed Pd–Rh catalysts on γ-Al2O3 support. Catalysis Today, 2014, 238, 80-86.	4.4	49
9	Effect of metal-metal and metal-support interaction on activity and stability of Pd-Rh/alumina in CO oxidation. Catalysis Today, 2017, 293-294, 73-81.	4.4	48
10	Catalytic Purification of Exhaust Gases Over Pd–Rh Alloy Catalysts. Topics in Catalysis, 2013, 56, 1008-1014.	2.8	47
11	Fluorinated cage multiwall carbon nanoparticles. Chemical Physics Letters, 2000, 322, 231-236.	2.6	46
12	Preferential CO oxidation over bimetallic Pt–Co catalysts prepared via double complex salt decomposition. Chemical Engineering Journal, 2012, 207-208, 683-689.	12.7	46
13	Vapour phase formic acid decomposition over PdAu/γ-Al2O3 catalysts: Effect of composition of metallic particles. Journal of Catalysis, 2013, 299, 171-180.	6.2	45
14	Thermal activation of Pd/CeO2-SnO2 catalysts for low-temperature CO oxidation. Applied Catalysis B: Environmental, 2020, 277, 119275.	20.2	43
15	Chemical vapor deposition and characterization of hafnium oxide films. Journal of Physics and Chemistry of Solids, 2008, 69, 685-687.	4.0	40
16	Creation of nanosized holes in graphene planes for improvement of rate capability of lithium-ion batteries. Nanotechnology, 2018, 29, 134001.	2.6	40
17	<i>In situ</i> synchrotron study of Au–Pd nanoporous alloy formation by single-source precursor thermolysis. Nanotechnology, 2012, 23, 405302.	2.6	37
18	Study of point defects in as-grown and annealed bismuth germanate single crystals. Journal of Applied Crystallography, 2005, 38, 448-454.	4.5	36

#	Article	IF	CITATIONS
19	Dimethylgold(III) carboxylates as new precursors for gold CVD. Surface and Coatings Technology, 2007, 201, 9099-9103.	4.8	35
20	Effect of Fe/Ni catalyst composition on nitrogen doping and field emission properties of carbon nanotubes. Carbon, 2008, 46, 864-869.	10.3	35
21	Double complex salts of Pt and Pd ammines with Zn and Ni oxalates – promising precursors of nanosized alloys. Inorganica Chimica Acta, 2008, 361, 199-207.	2.4	34
22	Bimetallic single-source precursors [M(NH3)4][Co(C2O4)2(H2O)2]·2H2O (M=Pd, Pt) for the one run synthesis of CoPd and CoPt magnetic nanoalloys. Polyhedron, 2011, 30, 1305-1312.	2.2	33
23	Silica, alumina and ceria supported Au–Cu nanoparticles prepared via the decomposition of [Au(en)2]2[Cu(C2O4)2]3·8H2O single-source precursor: Synthesis, characterization and catalytic performance in CO PROX. Catalysis Today, 2014, 235, 103-111.	4.4	33
24	Catalytic conversion of 1,2-dichloroethane over Ni-Pd system into filamentous carbon material. Catalysis Today, 2017, 293-294, 23-32.	4.4	32
25	Co-Pt bimetallic catalysts for the selective oxidation of carbon monoxide in hydrogen-containing mixtures. Kinetics and Catalysis, 2007, 48, 276-281.	1.0	30
26	Deposition of titanium dioxide from TTIP by plasma enhanced and remote plasma enhanced chemical vapor deposition. Surface and Coatings Technology, 2008, 202, 4076-4085.	4.8	30
27	One-step chemical vapor deposition synthesis and supercapacitor performance of nitrogen-doped porous carbon–carbon nanotube hybrids. Beilstein Journal of Nanotechnology, 2017, 8, 2669-2679.	2.8	30
28	Deposition of Au Thin Films and Nanoparticles by MOCVD. Chemical Vapor Deposition, 2012, 18, 336-342.	1.3	28
29	Synthesis of nanostructured carbon fibers from chlorohydrocarbons over Bulk Ni-Cr Alloys. Nanotechnologies in Russia, 2014, 9, 380-385.	0.7	28
30	Catalytic synthesis of carbon nanotubes using Ni- and Co-doped calcium tartrates. Carbon, 2009, 47, 1701-1707.	10.3	26
31	Successful synthesis and thermal stability of immiscible metal Au–Rh, Au–Ir andAu–Ir–Rh nanoalloys. Nanotechnology, 2017, 28, 205302.	2.6	26
32	Anisotropic properties of carbonaceous material produced in arc discharge. Applied Physics A: Materials Science and Processing, 2001, 72, 481-486.	2.3	25
33	Effect of Alumina Phase Transformation on Stability of Low-Loaded Pd-Rh Catalysts for CO Oxidation. Topics in Catalysis, 2017, 60, 152-161.	2.8	25
34	Effect of metal ratio in alumina-supported Pd-Rh nanoalloys on its performance in three way catalysis. Journal of Alloys and Compounds, 2018, 749, 155-162.	5.5	25
35	Nanoscale coupling of MoS2 and graphene via rapid thermal decomposition of ammonium tetrathiomolybdate and graphite oxide for boosting capacity of Li-ion batteries. Carbon, 2021, 173, 194-204.	10.3	25
36	Graphitization of 13C enriched fine-grained graphitic material under high-pressure annealing. Carbon, 2019, 141, 323-330.	10.3	24

#	Article	IF	CITATIONS
37	CO oxidation over fiberglasses with doped Cu-Ce-O catalytic layer prepared by surface combustion synthesis. Applied Surface Science, 2015, 349, 21-26.	6.1	23
38	Experimental redetermination of the Cu–Pd phase diagram. Journal of Alloys and Compounds, 2019, 777, 204-212.	5.5	23
39	The atomic and electron structure of ZrO2. Journal of Experimental and Theoretical Physics, 2006, 102, 799-809.	0.9	22
40	Growth of MoS2 layers on the surface of multiwalled carbon nanotubes. Inorganic Materials, 2007, 43, 236-239.	0.8	22
41	Chemical vapor deposition of Pd/Cu alloy films from a new single source precursor. Journal of Crystal Growth, 2015, 414, 130-134.	1.5	22
42	Formation of Active Sites of Carbon Nanofibers Growth in Self-Organizing Ni–Pd Catalyst during Hydrogen-Assisted Decomposition of 1,2-Dichloroethane. Industrial & Engineering Chemistry Research, 2019, 58, 685-694.	3.7	22
43	Effect of Mo on the catalytic activity of Ni-based self-organizing catalysts for processing of dichloroethane into segmented carbon nanomaterials. Heliyon, 2019, 5, e02428.	3.2	22
44	Determination of the equilibrium miscibility gap in the Pd–Rh alloy system using metal nanopowders obtained by decomposition of coordination compounds. Journal of Alloys and Compounds, 2015, 622, 1055-1060.	5.5	21
45	Promoting Effect of Co, Cu, Cr and Fe on Activity of Ni-Based Alloys in Catalytic Processing of Chlorinated Hydrocarbons. Topics in Catalysis, 2017, 60, 171-177.	2.8	21
46	Preparation of highly dispersed Ni1-xPdx alloys for the decomposition of chlorinated hydrocarbons. Journal of Alloys and Compounds, 2019, 782, 716-722.	5.5	20
47	Preparation and Properties of Thin HfO2 Films. Inorganic Materials, 2005, 41, 1300-1304.	0.8	19
48	Synthesis, crystal structure, and thermal properties of [Pd(NH3)4][AuCl4]2. Russian Journal of Inorganic Chemistry, 2007, 52, 371-377.	1.3	19
49	Ni-Cu and Ni-Co alloys: Synthesis, structure, and catalytic activity for the decomposition of chlorinated hydrocarbons. Inorganic Materials, 2014, 50, 566-571.	0.8	19
50	Hydrogen electrooxidation over palladium–gold alloy: Effect of pretreatment in ethylene on catalytic activity and CO tolerance. Electrochimica Acta, 2012, 76, 344-353.	5.2	18
51	Synthesis of unsaturated secondary amines by direct reductive amination of aliphatic aldehydes with nitroarenes over Au/Al <sub>2</sub> O <sub>3</sub> catalyst in continuous flow mode. RSC Advances, 2016, 6, 88366-88372.	3.6	18
52	Effect of Pd deposition procedure on activity of Pd/Ce0.5Sn0.5O2 catalysts for low-temperature CO oxidation. Catalysis Communications, 2016, 73, 34-38.	3.3	18
53	Peculiarity of Rh bulk diffusion in La-doped alumina and its impact on CO oxidation over Rh/Al2O3. Catalysis Communications, 2017, 97, 18-22.	3.3	18
54	Highâ€Pressure Highâ€Temperature Synthesis of MoS <sub>2</sub> /Holey Graphene Hybrids and Their Performance in Liâ€Ion Batteries. Physica Status Solidi (B): Basic Research, 2018, 255, 1700262.	1.5	18

#	Article	IF	CITATIONS
55	Structure and supercapacitor properties of few-layer low-fluorinated graphene materials. Journal of Materials Science, 2018, 53, 13053-13066.	3.7	18
56	Study of effect of thermal annealing on crystalline perfection of bismuth germanate single crystals grown by low thermal gradient Czochralski method. Zeitschrift Fur Kristallographie - Crystalline Materials, 2002, 217, .	0.8	17
57	Low-temperature oxidation of carbon monoxide on Pd(Pt)/CeO2 catalysts prepared from complex salts. Kinetics and Catalysis, 2011, 52, 282-295.	1.0	17
58	Effect of in-plane size of MoS2 nanoparticles grown over multilayer graphene on the electrochemical performance of anodes in Li-ion batteries. Electrochimica Acta, 2018, 283, 45-53.	5.2	17
59	Prospect of Using Nanoalloys of Partly Miscible Rhodium and Palladium in Three-Way Catalysis. Topics in Catalysis, 2019, 62, 305-314.	2.8	17
60	Perforation of graphite in boiling mineral acid. Physica Status Solidi (B): Basic Research, 2012, 249, 2620-2624.	1.5	16
61	Metal Ir coatings on endocardial electrode tips, obtained by MOCVD. Applied Surface Science, 2017, 425, 1052-1058.	6.1	16
62	The peculiarities of Au–Pt alloy nanoparticles formation during the decomposition of double complex salts. Journal of Alloys and Compounds, 2018, 740, 935-940.	5.5	16
63	Synthesis of bimetallic AuPt/CeO2 catalysts and their comparative study in CO oxidation under different reaction conditions. Reaction Kinetics, Mechanisms and Catalysis, 2019, 127, 69-83.	1.7	16
64	Title is missing!. Russian Chemical Bulletin, 2002, 51, 41-45.	1.5	15
65	Synthesis, crystal structures and thermal behavior of Ni(pda)(hfac)2 and Ni(pda)(thd)2 as potential MOCVD precursors (pda-1,3-diaminopropane, hfac-1,1,1,5,5,5-hexafluoro-2,4-pentanedionato(-),) Tj ETQq1 1 0.7	78443381.4 rg1	BT <b>10</b> verlock
66	Double complex salts [Pd(NH3)4]3[Rh(NO2)6]2, [Pd(NH3)4]3[Rh(NO2)6]2·H2O as promising precursors to prepare Pd-Rh nanoalloys. Journal of Structural Chemistry, 2012, 53, 527-533.	1.0	15
67	Catalytic synthesis of segmented carbon filaments via decomposition of chlorinated hydrocarbons on Ni-Pt alloys. Catalysis Today, 2020, 348, 102-110.	4.4	15
68	Synthesis of [M(NH3)5Cl](ReO4)2 (M = Cr, Co, Ru, Rh, Ir) and investigation of thermolysis products. Crystal structure of [Rh(NH3)5Cl](ReO4)2. Journal of Structural Chemistry, 2006, 47, 1103-1110.	1.0	14
69	Thermally exfoliated fluorinated graphite for NO <sub>2</sub> gas sensing. Physica Status Solidi (B): Basic Research, 2016, 253, 2492-2498.	1.5	14
70	The relationship between properties of fluorinated graphite intercalates and matrix composition. Journal of Thermal Analysis and Calorimetry, 2007, 90, 399-405.	3.6	13
71	Low temperature synthesis of Ru–Cu alloy nanoparticles with the compositions in the miscibility gap. Journal of Solid State Chemistry, 2014, 212, 42-47.	2.9	13
72	Multiscale characterization of 13C-enriched fine-grained graphitic materials for chemical and electrochemical applications. Carbon, 2017, 124, 161-169.	10.3	13

#	Article	IF	CITATIONS
73	Double complex salts [M(NH3)5Cl][M′Br4] (M = Rh, Ir, Co, Cr, Ru; M′ = Pt, Pd): Synthesis, x-ray diffraction characterization, and thermal properties. Russian Journal of Inorganic Chemistry, 2006, 51, 202-209.	1.3	12
74	Phase transitions of intercalation inclusion compounds C2F0.92Br0.0·yCH3CN in the temperature range 20–260°C. Journal of Structural Chemistry, 2006, 47, 1141-1154.	1.0	12
75	Heterometallic complexes of Co2+, Ni2+, and Zn2+ with the [RuNO(NO2)4OH]2â^' anion and pyridine: Synthesis, crystal structure, and thermolysis. Russian Journal of Coordination Chemistry/Koordinatsionnaya Khimiya, 2009, 35, 57-64.	1.0	12
76	Three new O,N-coordinated Ni(II) complexes: Syntheses, crystal structures, and MOCVD applications. Journal of Organometallic Chemistry, 2013, 741-742, 122-130.	1.8	12
77	Chlorination of perforated graphite via interaction with thionylchloride. Physica Status Solidi (B): Basic Research, 2014, 251, 2613-2619.	1.5	12
78	Purification of gasoline exhaust gases using bimetallic Pd–Rh/δ-Al2O3 catalysts. Reaction Kinetics, Mechanisms and Catalysis, 2019, 127, 137-148.	1.7	12
79	The equilibrium decomposition of Auî—,Pt solid solutions. Journal of the Less Common Metals, 1988, 142, 213-219.	0.8	11
80	Complex salts [Pd(NH3)4](ReO4)2 and [Pd(NH3)4](MnO4)2: Synthesis, structure, and thermal properties. Russian Journal of Coordination Chemistry/Koordinatsionnaya Khimiya, 2006, 32, 374-379.	1.0	11
81	Layered compounds based on perforated graphene. Journal of Structural Chemistry, 2011, 52, 903-909.	1.0	11
82	Magnetic anisotropy and order parameter in nanostructured CoPt particles. Applied Physics Letters, 2013, 103, .	3.3	11
83	Synthesis, crystal structures, and characterization of double complex salts [Au(en)2][Rh(NO2)6]·2H2O and [Au(en)2][Rh(NO2)6]. Journal of Molecular Structure, 2015, 1100, 174-179.	3.6	11
84	New SrPb3Br8 crystals: Growth, crystal structure and optical properties. Journal of Alloys and Compounds, 2016, 682, 832-838.	5.5	11
85	Iron-filled multi-walled carbon nanotubes for terahertz applications: effects of interfacial polarization, screening and anisotropy. Nanotechnology, 2018, 29, 174003.	2.6	11
86	Comparative study of 1,2-dichlorethane decomposition over Ni-based catalysts with formation of filamentous carbon. Catalysis Today, 2018, 301, 147-152.	4.4	11
87	Optical spectroscopy of Rh3+ ions in the lanthanum-aluminum oxide systems. Journal of Luminescence, 2018, 204, 609-617.	3.1	11
88	Interaction of Pd and Rh with ZrCeYLaO2 support during thermal aging and its effect on the CO oxidation activity. Reaction Kinetics, Mechanisms and Catalysis, 2020, 129, 117-133.	1.7	11
89	Effect of La Addition on the Performance of Three-Way Catalysts Containing Palladium and Rhodium. Topics in Catalysis, 2020, 63, 152-165.	2.8	11
90	Porosity and composition of nitrogen-doped carbon materials templated by the thermolysis products of calcium tartrate and their performance in electrochemical capacitors. Journal of Alloys and Compounds, 2021, 858, 158259.	5.5	11

#	Article	IF	CITATIONS
91	Facile synthesis of triple Ni-Mo-W alloys and their catalytic properties in chemical vapor deposition of chlorinated hydrocarbons. Journal of Alloys and Compounds, 2021, 866, 158778.	5.5	11
92	Synthesis and thermal decomposition of the oxalatho cuprates(II) – [M(NH <sub>3</sub> ) <sub>4</sub> ][Cu(C <sub>2</sub> O <sub>4</sub> ) <sub>2</sub> 2O, M = Pt, Pd. Zeitschrift Für Kristallographie, Supplement, 2007, 2007, 289-295.	0.5	11
93	XRD investigation and thermal properties of [Ir(NH3)6][Co(C2O4)3]•H2O and [Co(NH3)6][Ir(C2O4)3] — precursors for Co0.50Ir0.50. Zeitschrift Für Kristallographie, Supplement, 2009, 2009, 263-268.	0.5	11
94	Title is missing!. Journal of Structural Chemistry, 2002, 43, 649-655.	1.0	10
95	X-ray photoelectron spectroscopy study of intercalated compounds of fluorinated graphite C2FxBr0.01·yCH3CN. Journal of Structural Chemistry, 2006, 47, 930-938.	1.0	10
96	Relationship between properties of fluorinated graphite intercalates and matrix composition Part III. Intercalates with 1,2-dichloroethane. Journal of Thermal Analysis and Calorimetry, 2009, 96, 501-505.	3.6	10
97	XAFS investigation of [Pd(NH3)4][AuCl4]2 and its thermolysis products. Journal of Thermal Analysis and Calorimetry, 2010, 102, 703-708.	3.6	10
98	Structure of platinum coatings obtained by chemical vapor deposition. Journal of Structural Chemistry, 2015, 56, 1215-1219.	1.0	10
99	Carbon Nanotube Synthesis Using Feâ€Mo/MgO Catalyst with Different Ratios of CH <sub>4</sub> and H <sub>2</sub> Gases. Physica Status Solidi (B): Basic Research, 2018, 255, 1700274.	1.5	10
100	Synthesis of Filamentary Carbon Material on a Self-Organizing Ni–Pt Catalyst in the Course of 1,2-Dichloroethane Decomposition. Kinetics and Catalysis, 2018, 59, 363-371.	1.0	10
101	Synthesis and Study of Bimetallic Pd-Rh System Supported on Zirconia-Doped Alumina as a Component of Three-way Catalysts. Emission Control Science and Technology, 2019, 5, 363-377.	1.5	10
102	Pressureâ€Assisted Interface Engineering in MoS <sub>2</sub> /Holey Graphene Hybrids for Improved Performance in Liâ€ion Batteries. Energy Technology, 2019, 7, 1900659.	3.8	10
103	Optical Spectroscopy Methods in the Estimation of the Thermal Stability of Bimetallic Pd–Rh/Al2O3 Three-Way Catalysts. Topics in Catalysis, 2019, 62, 296-304.	2.8	10
104	The Attractiveness of the Ternary Rh-Pd-Pt Alloys for CO Oxidation Process. Processes, 2020, 8, 928.	2.8	10
105	X-ray diffraction reinvestigation of the Ni-Pt phase diagram. Journal of Alloys and Compounds, 2022, 891, 161974.	5.5	10
106	Preparation of porous Co-Pt alloys for catalytic synthesis of carbon nanofibers. Nanotechnology, 2020, 31, 495604.	2.6	10
107	MO CVD obtaining composite coatings from metal of platinum group on titanium electrodes. European Physical Journal Special Topics, 2001, 11, Pr3-593-Pr3-599.	0.2	9
108	X-ray study of the thermolysis products of (NH4)2[OsCl6] x [PtCl6]1â^'x. Journal of Structural Chemistry, 2009, 50, 1121-1125.	1.0	9

#	Article	IF	CITATIONS
109	Effect of the nature of a textural promoter on the catalytic properties of a nickel-copper catalyst for hydrocarbon processing in the production of carbon nanofibers. Catalysis in Industry, 2014, 6, 176-181.	0.7	9
110	Mechanochemical Synthesis, Structure, and Catalytic Activity of Ni-Cu, Ni-Fe, and Ni-Mo Alloys in the Preparation OF Carbon Nanofibers During the Decomposition of Chlorohydrocarbons. Journal of Structural Chemistry, 2020, 61, 769-779.	1.0	9
111	Carbon Erosion of a Bulk Nickel–Copper Alloy as an Effective Tool to Synthesize Carbon Nanofibers from Hydrocarbons. Kinetics and Catalysis, 2022, 63, 97-107.	1.0	9
112	Equilibrium solid solubilities in the Ag-Cu system by X-ray diffractometry. Journal of Physics F: Metal Physics, 1988, 18, 2381-2386.	1.6	8
113	[M(NH3)5Cl][AuCl4]Cl · nH2O (M = Rh, Ru, or Cr): Synthesis, crystal structure, and thermal properties. Russian Journal of Inorganic Chemistry, 2008, 53, 1724-1732.	1.3	8
114	Composites based on polyaniline and aligned carbon nanotubes. Polymer Science - Series B, 2010, 52, 101-108.	0.8	8
115	The relationship between properties of fluorinated graphite intercalates and matrix composition. Journal of Thermal Analysis and Calorimetry, 2010, 100, 163-169.	3.6	8
116	Synergetic effect in PdAu/CeO2 catalysts for the low-temperature oxidation of CO. Journal of Structural Chemistry, 2011, 52, 123-136.	1.0	8
117	The exchange interaction effects on magnetic properties of the nanostructured CoPt particles. Journal of Magnetism and Magnetic Materials, 2016, 401, 236-241.	2.3	8
118	Catalytic behavior of bimetallic Ni–Fe systems in the decomposition of 1,2-dichloroethane. Effect of iron doping and preparation route. Reaction Kinetics, Mechanisms and Catalysis, 2017, 121, 413-423.	1.7	8
119	Synthesis of Porous Nanostructured MoS2 Materials in Thermal Shock Conditions and Their Performance in Lithium-Ion Batteries. ACS Applied Energy Materials, 2020, 3, 10802-10813.	5.1	8
120	Room temperature synthesis of fluorinated graphite intercalation compounds with low fluorine loading of host matrix. Journal of Fluorine Chemistry, 2020, 232, 109482.	1.7	8
121	Redox reactions between acetonitrile and nitrogen dioxide in the interlayer space of fluorinated graphite matrices. Physical Chemistry Chemical Physics, 2021, 23, 10580-10590.	2.8	8
122	Equilibrium decomposition curve of Auî—,Ni solid solutions. Journal of the Less Common Metals, 1989, 155, 319-326.	0.8	7
123	Synthesis, structure, and thermal transformations of double complex salts [Au(C4H13N3)Cl][MCl6]Â∙ nH2O (M = Ir, Pt; n = 0–2). Russian Chemical Bulletin, 2006, 55, 429-434.	1.5	7
124	Double complex salts [Pt(NH3)5Cl][M(C2O4)3] · nH2O (M = Fe, Co, Cr): Synthesis and study. Russian Journal of Inorganic Chemistry, 2007, 52, 1487-1491.	1.3	7
125	Phase states and magnetic properties of iron nanoparticles in carbon nanotube channels. Journal of Experimental and Theoretical Physics, 2009, 109, 254-261.	0.9	7
126	Structure of Ir and Ir-Al2o3 coatings obtained by chemical vapor deposition in the presence of oxygen. Journal of Structural Chemistry, 2010, 51, 82-91.	1.0	7

#	Article	IF	CITATIONS
127	Bimetallic Pt,Ir-containing coatings formed by MOCVD for medical applications. Journal of Materials Science: Materials in Medicine, 2019, 30, 69.	3.6	7
128	One-pot functionalization of catalytically derived carbon nanostructures with heteroatoms for toxic-free environment. Applied Surface Science, 2022, 590, 153055.	6.1	7
129	Water purification from chlorobenzenes using heteroatom-functionalized carbon nanofibers produced on self-organizing Ni-Pd catalyst. Journal of Environmental Chemical Engineering, 2022, 10, 107873.	6.7	7
130	On the constancy of the "average―crystal lattice parameter in the decay of the solid solutions PbS î—, PbTe. Materials Research Bulletin, 1984, 19, 1355-1359.	5.2	6
131	High-temperature X-ray diffraction study of thermolysis of the double complex salt [Rh(NH3)5Cl][PtCl4]. Russian Chemical Bulletin, 2006, 55, 1109-1113.	1.5	6
132	Crystal structure of [Pd(NH3)4][Rh(NH3)(NO2)5]. Journal of Structural Chemistry, 2011, 52, 621-624.	1.0	6
133	Crystal structure of [Pd(NH3)4]3[Ir(NO2)6]2·H2O. Journal of Structural Chemistry, 2011, 52, 816-819.	1.0	6
134	Deposition of Ni thin films from Ni(II) $\hat{l}^2$ -diketonates derivatives with 1,3-diaminopropane. Journal of Physics and Chemistry of Solids, 2013, 74, 1204-1211.	4.0	6
135	Synthesis of a bismuth germanium oxide source material for Bi4Ge3O12 crystal growth. Inorganic Materials, 2013, 49, 412-415.	0.8	6
136	Thermal decomposition of [Co(NH3)6][Fe(C2O4)3]•3H2O in inert and reductive atmospheres. Russian Chemical Bulletin, 2015, 64, 1963-1966.	1.5	6
137	Effect of Hot Pressing on the Electrochemical Performance of Multilayer Holey Graphene Materials in Liâ€ion Batteries. Physica Status Solidi (B): Basic Research, 2018, 255, 1800202.	1.5	6
138	Adsorption of 1,2-Dichlorobenzene on a Carbon Nanomaterial Prepared by Decomposition of 1,2-Dichloroethane on Nickel Alloys. Russian Journal of Applied Chemistry, 2020, 93, 1873-1882.	0.5	6
139	Metal dusting as a key route to produce functionalized carbon nanofibers. Reaction Kinetics, Mechanisms and Catalysis, 2022, 135, 1387-1404.	1.7	6
140	Catalytic Properties of Bulk (1–x)Ni–xW Alloys in the Decomposition of 1,2-Dichloroethane with the Production of Carbon Nanomaterials. Kinetics and Catalysis, 2022, 63, 75-86.	1.0	6
141	Title is missing!. Journal of Structural Chemistry, 2002, 43, 643-648.	1.0	5
142	Fluorination of CN x Nanotubes. Fullerenes Nanotubes and Carbon Nanostructures, 2005, 12, 99-104.	2.1	5
143	Re-determination of the crystal structure and investigation of thermal decomposition of the Chugaev's salt, [Pt(NH3)5Cl]Cl3·H2O. Journal of Structural Chemistry, 2006, 47, 735-739.	1.0	5
144	Complex salts (DienH3)[IrCl6](NO3), (DienH3)[PtCl6](NO3), and (DienH3)[IrCl6]0.5[PtCl6]0.5(NO3): Synthesis, structure, and thermal properties. Russian Journal of Coordination Chemistry/Koordinatsionnaya Khimiya, 2007, 33, 45-52.	1.0	5

#	Article	IF	CITATIONS
145	Growth of carbon nanotubes via chemical vapor deposition on Co catalyst nanoparticles dispersed in CaO. Inorganic Materials, 2008, 44, 213-218.	0.8	5
146	Crystal structure and thermal properties of [Au(en)2]2[Cu(C2O4)2]3·8H2O. Journal of Structural Chemistry, 2011, 52, 924-929.	1.0	5
147	Formation of Mo <sub>2</sub> S <sub>3</sub> Layers on the Surface of Graphitic Platelets. Key Engineering Materials, 0, 508, 56-60.	0.4	5
148	Copper–Palladium Phase Diagram. Russian Journal of Inorganic Chemistry, 2021, 66, 891-893.	1.3	5
149	Bromination of carbon nanohorns to improve sodium-ion storage performance. Applied Surface Science, 2022, 580, 152238.	6.1	5
150	On the "average―crystal lattice parameter in decomposition of CsBrî—,CsJ solid solutions. Journal of Solid State Chemistry, 1987, 67, 191-196.	2.9	4
151	Correlation of the structural imperfection and morphology of Bi4Ge3O12 crystals grown by the low-gradient Czochralski method. Crystallography Reports, 2004, 49, 175-179.	0.6	4
152	[Zn(NH3)4][PtCl6] and [Cd(NH3)4][PtCl6] as precursors for intermetallic compounds PtZn and PtCd. Russian Journal of Inorganic Chemistry, 2007, 52, 500-504.	1.3	4
153	X-ray powder diffraction study of the products of thermobaric treatment of the Re0.67Rh0.33 solid solution. Journal of Structural Chemistry, 2008, 49, 47-52.	1.0	4
154	Formation of nanosized bimetallic particles based on noble metals. Catalysis in Industry, 2010, 2, 20-25.	0.7	4
155	Bimetallic Au-Cu/CeO2 catalyst: Synthesis, structure, and catalytic properties in the CO preferential oxidation. Catalysis in Industry, 2014, 6, 36-43.	0.7	4
156	MOCVD growth of Pt films using a novel Pt(IV) compound as a precursor. Physica Status Solidi C: Current Topics in Solid State Physics, 2015, 12, 1053-1059.	0.8	4
157	MOCVD growth and study of magnetic Co films. Surface Engineering, 2016, 32, 8-14.	2.2	4
158	Structural rearrangements of the first stage inclusion compound of fluorinated graphite with acetonitrile during isothermal deintercalation. Journal of Thermal Analysis and Calorimetry, 2017, 128, 349-355.	3.6	4
159	Transformation of alumina-supported Pt-Au alloyed nanoparticles into core-shell Pt@Au structures during high-temperature treatment. Journal of Nanoparticle Research, 2020, 22, 1.	1.9	4
160	Sodium storage properties of thin phosphorus-doped graphene layers developed on the surface of nanodiamonds under hot pressing conditions. Fullerenes Nanotubes and Carbon Nanostructures, 2020, 28, 335-341.	2.1	4
161	COMPLEX SALT [Pd(NH3)4][Pd(NH3)3NO2][RhOx3]·H2O AS A PROSPECTIVE PRECURSOR OF Pd–Rh NANOALLOYS. CRYSTAL STRUCTURE OF Na3[RhOx3]·4H2O. Journal of Structural Chemistry, 2021, 62, 782-793.	1.0	4
162	Study of nanoalloys formation mechanism from single-source precursors [M(NH <sub>3</sub> ) <sub>5</sub> Cl](ReO <sub>4</sub> ) <sub>2</sub> , M = Rh, Ir. Zeitschrift Für Kristallographie, Supplement, 2007, 2007, 283-288.	0.5	4

#	Article	IF	CITATIONS
163	Interaction of chlorinated hydrocarbons with nichrome alloy: From surface transformations to complete dusting. Surfaces and Interfaces, 2022, 30, 101914.	3.0	4
164	Synthesis and crystal structure of [Cr(NH3)5Cl][PdCl4]�H2O. Journal of Structural Chemistry, 2004, 45, 523-526.	1.0	3
165	Investigation of phase interactions in C60 fullerite films during gas phase metal deposition. Journal of Structural Chemistry, 2004, 45, S76-S83.	1.0	3
166	The structural characteristics and homogeneity regions of solid phases in the digraphite fluoride-acetonitrile system. Russian Journal of Physical Chemistry A, 2006, 80, 1198-1204.	0.6	3
167	The relationship between properties of fluorinated graphite intercalates and matrix composition. Journal of Thermal Analysis and Calorimetry, 2011, 104, 1077-1082.	3.6	3
168	Synthesis of bimetallic nanocompositions AuxPd1-x/γ-Al2O3 for catalytic CO oxidation. Journal of Nanoparticle Research, 2017, 19, 1.	1.9	3
169	Double complex salts [Au(En)2][Ir(NO2)6] • nH2O (n = 0, 2), [Au(En)2][Ir(NO2)6] x [Rh(NO2)6]1–x • nH (x = 0.25, 0.5, 0.75): Synthesis, structure, thermal properties. Russian Journal of Inorganic Chemistry, 2017, 62, 12-21.	20 1.3	3
170	New Trends in Automotive Exhaust Gas Purification Materials: Improvement of the Support against Stability of the Active Components. Materials Science Forum, 0, 950, 185-189.	0.3	3
171	Synthesis of nitrogen doped segmented carbon nanofibers via metal dusting of Ni-Pd alloy. Catalysis Today, 2020, 388-389, 312-312.	4.4	3
172	Magnetic Properties of 1D Iron–Sulfur Compounds Formed Inside Singleâ€Walled Carbon Nanotubes. Physica Status Solidi - Rapid Research Letters, 2020, 14, 2000291.	2.4	3
173	X-ray diffraction investigations of Ag2ReCl6 and Ag2OsCl6. Russian Chemical Bulletin, 2000, 49, 1310-1312.	1.5	2
174	The study on electro-physical properties of sandwich structures based on fullerite films. , 0, , .		2
175	Thermodynamic Approach to Optimization of SrTiO <sub>3</sub> Chemical Vapor Deposition from Volatile Metalorganic Precursors. Inorganic Materials, 2004, 40, 516-521.	0.8	2
176	Synthesis of CNx nanotubes using catalysts prepared from zinc and nickel bimaleates. Inorganic Materials, 2007, 43, 945-950.	0.8	2
177	The role of intermolecular interactions in structure formation of host guest inclusion compounds based on a graphite fluoride polymer matrix. Journal of Structural Chemistry, 2009, 50, 754-760.	1.0	2
178	Formation of solid solutions in the Re-Rh system upon thermobaric treatment of nanosized metal powders. Journal of Structural Chemistry, 2011, 52, 505-509.	1.0	2
179	Domain structure of Colr nanoalloys. Powder Diffraction, 2017, 32, S155-S159.	0.2	2
180	Design of Nanoalloyed Catalysts for Hydrogen Production Processes. Nanobiotechnology Reports, 2021, 16, 195-201.	0.6	2

#	Article	IF	CITATIONS
181	In situsynchrotron X-ray diffraction study of formation mechanism of Rh0.33Re0.67nanoalloy powder upon thermal decomposition of complex precursor. Zeitschrift Für Kristallographie, Supplement, 2008, 2008, 185-192.	0.5	2
182	Experimental investigation of phase equilibria of the Ir-Pt binary system in subsolidus region. Materials Today Communications, 2022, 31, 103247.	1.9	2
183	Synthesis and Structure of Binary Complexes of Platinum Group Metals - Precursors of Metallic Materials. ChemInform, 2004, 35, no.	0.0	1
184	Synthesis and characterization of [Co(NH3)5NO2][M(NO2)4] (M = Pt, Pd) compounds and their thermolysis products. Russian Journal of Inorganic Chemistry, 2006, 51, 521-530.	1.3	1
185	Investigation of thermal properties of double complex salts [M(NH3)5Br][AuBr4]2·nH2O, MÂ=ÂRh, Ir. Journal of Thermal Analysis and Calorimetry, 2012, 109, 901-905.	3.6	1
186	Chemical Composition, Structure, and Functional Properties of the Coatings of Microchannel Plate Channels. Journal of Surface Investigation, 2019, 13, 451-455.	0.5	1
187	Single-source heterometallic precursors to MOCVD Pd Cu alloy films for energy and catalysis applications. , 2022, , 453-472.		1
188	COMPLEX SALTS [Pd(NH3)4][Pd(NH3)3NO2] [CrOx3]·H2O AND [Pd(NH3)4][Pd(NH3)3NO2] [CoOx3]·H2O A SOLID SOLUTIONS [Pd(NH3)4] [Pd(NH3)3NO2][CoOx3]x[RhOx3]1–x·H2O : PROMISING PRECURSORS FOR POROUS NANOALLOYS. Journal of Structural Chemistry, 2022, 63, 556-568.	ND 1.0	1
189	Clathrate formation and phase equilibria in the thiourea-bromoform system. Russian Journal of Physical Chemistry A, 2008, 82, 1061-1065.	0.6	0
190	Phase equilibria in the thiourea-benzene system. Russian Journal of Physical Chemistry A, 2009, 83, 724-728.	0.6	0
191	Synthesis and properties of (C2F x Br0.01 · y CH3COOC2H5) n (0.5 < x < 1.0) intercalation compounds. Inorganic Materials, 2013, 49, 528-533.	0.8	0
192	Ordering and magnetic properties of nanostructured CoPt particles. Bulletin of the Russian Academy of Sciences: Physics, 2017, 81, 298-300.	0.6	0
193	Partial Miscibility of Metals as a Key for Improved Properties. Materials Science Forum, 2020, 998, 151-156.	0.3	0
194	SYNTHESIS, STRUCTURE, AND THERMAL PROPERTIES OF DOUBLE COMPLEX SALTS AS PRECURSORS OF NANOALLOYS OF IMMISCIBLE METALS. Journal of Structural Chemistry, 2022, 63, 353-377.	1.0	0